Fall 8-19-2013

A Study on Several Applications for Impulse Force Supporting Technique and the Controlling Problem

Dalong An

A STUDY ON SEVERAL APPLICATIONS FOR IMPULSE FORCE SUPPORTING TECHNIQUE AND THE CONTROLLING PROBLEM

by

DALONG AN

A thesis submitted in partial fulfillment
of the requirements for the degree of
Master's degree in Mathematics

Department of Mathematics
Reagan Beckham, Ph.D., Committee Chair
College of Arts and Sciences

The University of Texas at Tyler
May 2013

The University of Texas at Tyler
Tyler, Texas
This is to certify that the Master's Thesis/Doctoral Dissertation of

DALONG AN

has been approved for the thesis requirement on
23/4/2013
for the Master's degree in Mathematics

Approvals:

Thesis Chair: Reagan Beckham, Ph.D.

Member: Deborah Koslover, Ph.D.

Member: Nathan Smith, Ph.D.

Chair, Department of Mathematics

Dean, College of Arts and Sciences

Contents

List of Figures

Abstract

A STUDY ON SEVERAL APPLICATIONS FOR IMPULSE FORCE SUPPORTING TECHNIQUE AND THE CONTROLLING PROBLEM

Dalong An

Thesis Chair: Reagan Beckham, Ph.D.

University of Texas at Tyler

May 2013

Motivated by the Space Elevator concept, several alternate space transportation systems are studied. Details, such as the structure, transporting capacity, and stability of the systems are explored. Further study shows that despite the difference in their structure, these transportation systems are all applications for the impulse force supporting technique. Moreover, we can show that the centrifugal force and the impulse force are merely two aspects of one kind of supporting force, each 1of which can be used for different purposes.

1 Introduction

In the 20th century rocket science made space exploration a reality. However, as our desire for developing in outer space grows with time, rocket-based space transportation is becoming less and less efficient. Projects like the Space Station or human's landing on Mars require a more efficient space transportation system. The Space Elevator is one of the most popular ideas for alternate space transportation systems. Unfortunately, the Space Elevator has many problems. The most fatal one is the lack of strong materials for an extremely long tether (we will address this problem more in Chapter 2 Section 1). Rather than waiting for material scientists to come up with a super strong material capable of this, some scientists suggest reconstructing the Space Elevator such that a super strong tether is no longer needed, hence the design of the Orbital Ring System, the Partial Orbital Ring System, the Lofstrom Launch Loop, and the Space Cable. Despite their minor differences in structure, the supporting forces they use are the same to some extent. In this paper, we refer to this force as the impulse momentum supporting force. All these impulse momentum supporting force based systems have their own problems as well, some of which will be addressed in this paper. We start our discussion with the Orbital Ring System, the very first application of the impulse supporting technique.

2 Orbital Ring System

2.1 Space Elevator & Orbital Ring System

The Orbital Ring System, ORS for short, was the first application of

the impulse force supporting technique. It was proposed by Paul Birch, from 1981 to 1982 [Birch, 1982, 1983a,b]. The ORS was proposed as a solution to a problem concerning an existing engineering project, the Space Elevator. In order to gain a better understanding of the ORS, it is beneficial to introduce some background on the Space Elevator.

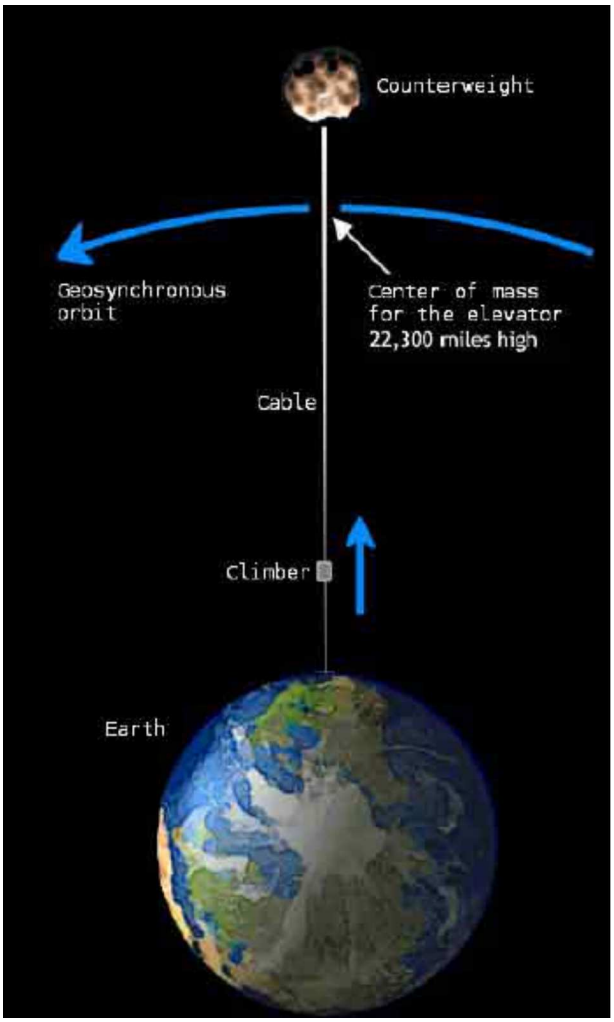

Figure 1: An illustration for the Space elevator

A Space Elevator, see Figure 1, is a large scale space transportation system. Its main component is a lifting cable (also called a tether) with its bottom end anchored to the surface, and the top end extending beyond the geosynchronous orbit, where it is attached to a

counter-weight (a relatively massive object). Although the orbit of the counter-weight is higher than the Geo-synchronous orbit, it rotates with an angular speed same to that of the Earth. Because of this, the lifting cable will be stretched and the tension force inside the cable will provide the additional centripetal force needed to prevent the counter-weight from ascending to a higher orbit. As a result, the tension force inside the cable allows the climber to move along the cable, and thereby bring cargo into space.

It is not difficult to see that there are many problems concerning the Space Elevator, such as the deployment, meteorite damage, or weather disturbance. One of the most fatal problems is the extremely high altitude of the geosynchronous orbit. The lifting cable of the Space Elevator has to reach and even go beyond the geosynchronous orbit, therefore the cable is much too heavy to keep itself from being torn to pieces by its own weight. Existing materials are far from strong enough to be made into the lifting cable. Although in the 1990s the discovery of the carbon nanotube once brought hope to this problem, a major breakthrough in carbon nanotube research is still needed, before we can confidently claim that the Space Elevator is theoretically and economically feasible.

2.2 ORS

Some researchers decided to move on and avoid the problems found in the Space Elevator by changing the structure, so that the requirements for the strength of the lifting cable can be reduced. The ORS is a good example of this.

The ORS consists of four major parts:

1) Orbital ring: A ring-shaped cable or particle flow, rotating fast above the surface of the Earth with the Earth at its center. Its main job is to provide the impulse force, thereby supporting the whole structure. It is important to point out that the orbital ring is not necessarily a circle or any smooth conic curve like the shape of the orbits of the satellites. Rather, an orbital ring is pieced together by several conic shaped cables, each piece is a smooth conic curve. At each joining point, the cable makes a sharp turn due to an impulse.

2) Jacob's ladder: Jacob's ladder is a lifting cable that allows the cargo to climb. Compared to the lifting cable in the Space Elevator, Jacob's ladder is much shorter. The lifting cable in the Space Elevator can be as long as 36000km, but a Jacob's ladder is only 300 to 500km long. Another major difference between Jacob's ladder and the tether in the Space Elevator is the Skyhook, which is a floating device that connects the ladder and lifting cable together.

3) Skyhook: The connecting device between the orbital ring and the ladder. As we have mentioned above, the Orbital Ring always rotates around the Earth, whereas Jacob's ladder stays relatively stationary to the ground. Therefore, instead of being connected to both of them, the Skyhook is directly fixed only to the ladder, and with the help of some super conductive device, it floats above the surface of the orbital ring.

4) Earth base: The port and controlling base. All the climbers start their trips from the Earth base, bringing cargo into space.

With the structure of ORS in mind, the following is the basic physical scenario for the impulse between the Orbital Ring and the Skyhook, which generate the lifting force.

2.2.1 The Motion of the Orbital Ring

The Orbital Ring moves in elliptic orbits instead of circular orbits. Instead of following one single elliptic orbit, the Orbital Ring continually switches from one orbit to another. The following image shows an Orbital Ring with 4 elliptic orbits.

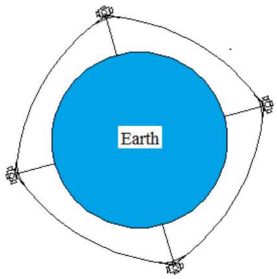

Figure 2: Orbital Ring with 4 elliptic orbits

In Figure 2, the straight vertical lines represent the lifting cables, and the curves around the Earth represent the Orbital Ring. An orbital ring can be continuous or discontinuous, but for our study, we assume it to be continuous. Although the orbital ring is continuous, it apears to be like pieced together by several discontinuous segments. This can be further explained by Figure 3.

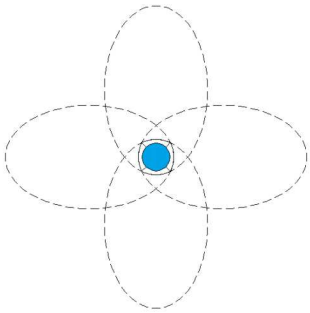

Figure 3: A more direct impression of the orbit change of the orbital ring

We can see, each "piece" of the orbital ring belongs to a different elliptic orbit, and it will constantly switch its orbit from one to another as they rotate around the Earth. Additionally, we see that orbit switching occurs at the Skyhook, when the orbital ring impacts the Skyhook from below. In order to gain a better understanding, we study the impulse scenario by picking an arbitrary short segment of the Orbital Ring, see Figure 4.

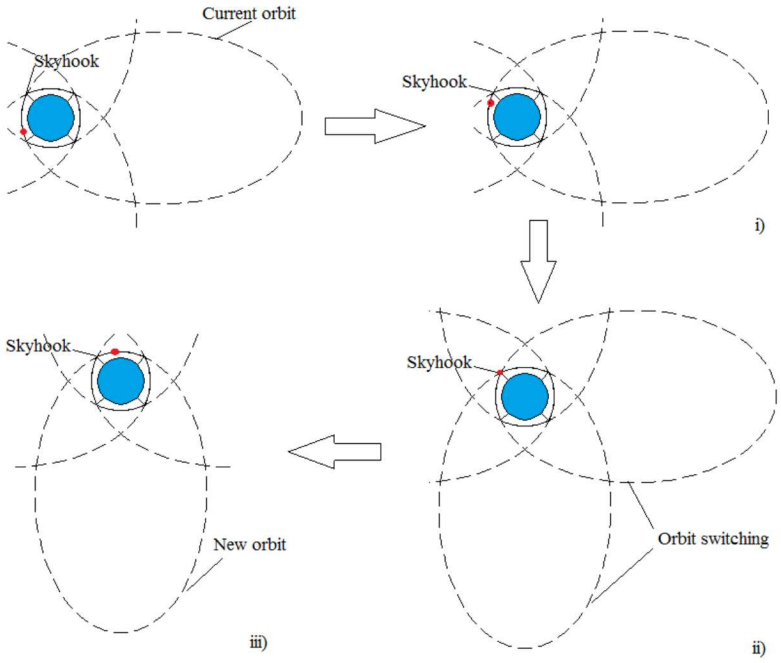

Figure 4: The Motion of a Segment

In Figure 4 we see a red dot moving along the orbital ring. This red dot represents the short segment that travels along some elliptic orbit. In Figure 4 i), the segment travels along the current elliptical orbit until it reaches the Skyhook. When the segment reaches the Skyhook, it will impact the Skyhook, and therefore be turned by a small angle, see ii). Since the segment has been suddenly turned by a small angle, it will enter into another elliptical orbit, see iii). Repeating this process, the segment will constantly switch orbits around the Earth, and finally return to its original orbit, forming a complete loop. Moreover, since the Orbital Ring is comprised by infinitely many such segments, there will always be some segment impacting the Skyhook. This will provide a constant impulse force that can be used to support the weight of the Skyhook, Jacob's ladder and the climber on it. With a first impression of the motion of the orbital ring, we are now ready to discuss the mathematical details behind it. The purpose of the ORS is to lift cargo into space. The lifting capacity is determined by many parameters, such as the velocity of the orbital ring, the turning angle, etc.

According to [Birch, 1982], the equation

$$F_I = mv_0^2\Delta\theta \tag{1}$$

describes the basic lifting force of the ORS. Here F_I is the impulse force that can be used to lift cargo, m is the linear density of the ring, v_0 is the velocity of the mass flowing pass the Skyhook and $\Delta\theta$ is the velocity change at Skyhook. The linear density is ρA, where ρ is the mass

density per volume and A is the cross-section area. To see this, consider a short period dt, during which a small fragment of the cylindrical orbital ring cable, with mass mdl, impacts the Skyhook with velocity v_0. The impact force, F_I, between this fragment of orbital ring and the Skyhook can be expressed, according to the theorem of momentum impulse as[1]

$$\begin{aligned} F_I dt &= (mdl)v_0 \sin\Delta\theta \\ F_I &= \left(m\frac{dl}{dt}\right) v_0 \sin\Delta\theta \\ &= (mv_0)v_0 \sin\Delta\theta \end{aligned}$$

Assuming the turning angle is small, we can expend $\sin\Delta\theta$ with respect to $\Delta\theta$, obtainning $\sin\Delta\theta = \Delta\theta - (\Delta\theta^3/3!) + (\Delta\theta^5/5!) - .....$ Using this we approximate that$\sin\Delta\theta \approx \Delta\theta$, giving Equation (1).

2.2.2 The Geometric Parameters In ORS

It seems that there are three major factors that determine the lifting ability of ORS. First is the mass of the Orbital Ring, second is its velocity, and third is the velocity change. These are not totally independent of one another, since the total number of Skyhooks would affect the shape of the orbital ring. Equation (1) is simply an impact scenario. There is no parameter concerning the geometric shape of the

[1] $\Delta p = Fdt$, an impulse force delivered to a particle object will change its momentum [Knight, 2007]

orbital ring. Therefore, taking the geometric parameters of the shape of the ring into consideration, we have

$$F_I = \frac{4mgR^2\Delta H}{\alpha(R+H)(R+H+\Delta H(1-2/\alpha^2))}. \tag{2}$$

Next we shall deduce this equation. Before doing this, we introduce the meaning of the geometric parameters and give more background for the Skyhook.

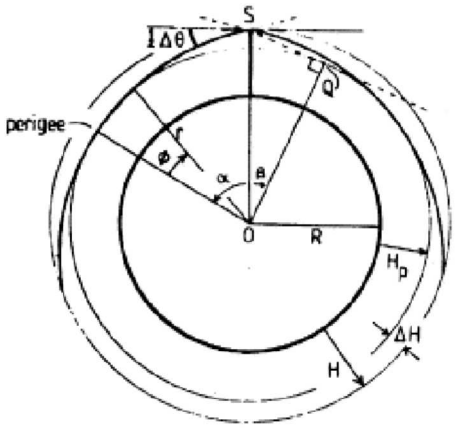

Figure 5: The parameters describing the shape of the Orbital Ring [Birch, 1982]

Figure 5 gives an illustration of the important parameters that determine the shape of the orbital ring. Here S stands for the location of the Skyhook. The orbital ring changes its direction at the Skyhook, forming a "hump". This is the place where the Orbital Ring changes its orbit from one eccentric orbit to another. The more Skyhooks in ORS, the more circle-like the Orbital Ring will be. Each Skyhook corresponds to a part of eccentric orbit, and each pair of the eccentric orbits will be

pieced together at the Skyhooks. Figure 6, according to [Birch, 1982], illustrates the orbit changing process of an ORS with 2 Skyhooks:

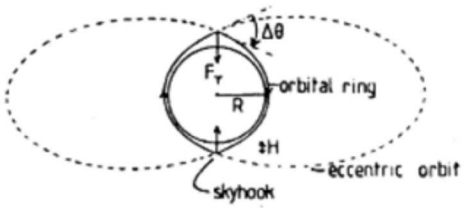

Figure 6: The orbit changing process
[Birch, 1982]

The Skyhook is one of the most important devices of ORS. It allows the orbital ring to flow through from inside, and also connect the lifting cable from outside. The super-conducting device can keep the Skyhooks floating above the surface of the ring. Figure 7 gives both a cross-section and side view of the Skyhook.

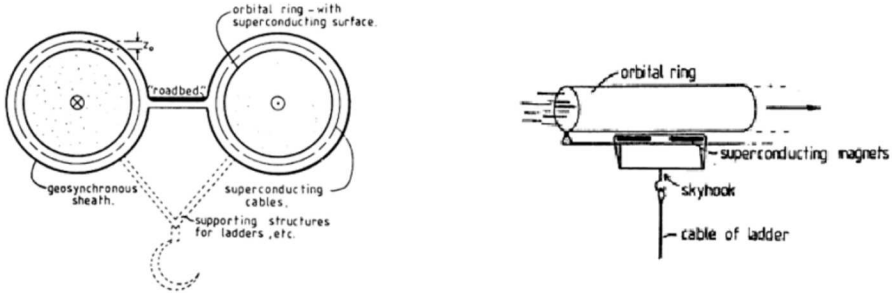

Figure 7: The image of the Skyhook
Birch [1982]

Now we move on and deduce Equation (2), which is one of the most important equations in the theory of ORS, since it shows us the

relationship between the lifting capacity of the ORS and the initial condition of the ORS design. In Figure 5, we have an arbitrary Skyhook and two pieces of the Orbital Ring that move towards it and away from it respectively. S represents the location of Skyhook, and $\Delta\theta$ is the turning angle of the orbital ring. The perigee tag represents the perigee point of the left hand side Orbital Ring. The height of the perigee point is H_p, and the height of the Skyhook is H. The center angle between the perigee point and the Skyhook is α, and R represents the radius of the Earth. Since each piece of the orbital ring is theoretically conic, the following conic polar function describes the shape of each piece of the orbital ring

$$1/r = a\cos\phi + b. \tag{3}$$

In order to determine the constants a,b respectively, apply the boundary condition at the perigee point, where $\phi = 0$, and
$r = R + H_p = R + H - \Delta H$. We get

$$\frac{1}{R + H - \Delta H} = a + b. \tag{4}$$

Also, applying the boundary condition at the Skyhook, i.e. the S point,

where $\phi = \alpha$, and $r = R + H$, gives

$$\frac{1}{R+H} = a\cos\alpha + b. \tag{5}$$

Next we compute the slope relative to the local vertical. Consider a point on the orbital ring, which travels as the orbital ring rotates. Let the point travel by a small angle $d\phi$, then $rd\phi$ is the arc length of arc that this point travels through. Since we assume the orbit is smooth, a small change in angle corresponds to a small change of the arc radius. The change of the radius is given by dr. Therefore we have the slope of the local vertical to be $dr/(rd\phi)$. Substituting the result from Equation (4) we obtain

$$\begin{aligned}\frac{1}{r}\cdot\frac{dr}{d\phi} &= \frac{1}{r}\cdot d(\frac{1}{a\cos\phi+b})/d\phi \\ &= (a\cos\phi+b)\frac{a\sin\phi}{(a\cos\phi+b)^2} \\ &= \frac{a\sin\phi}{a\cos\phi+b}\end{aligned}$$

$$\frac{1}{r}\cdot\frac{dr}{d\phi} = a\sin\phi/(a\cos\phi+b). \tag{6}$$

Referring to Figure 5, "S" is where the Skyhook is located. The orbital ring impacts the Skyhook, and thereby is turned by $\Delta\theta$. The local vertical slope is given by $\tan\Delta\theta/2$, and we have

$$\tan(\Delta\theta/2) = a\sin\alpha/(a\cos\alpha+b). \tag{7}$$

We now use Equations (4) and (5), to represent a, and b, using R, H, ΔH. First find a

$$\begin{aligned} a - a\cos\alpha &= \frac{1}{R+H-\Delta H} - \frac{1}{R+H} \\ a(1-\cos\alpha) &= \frac{\Delta H}{(R+H-\Delta H)(R+H)} \\ a &= \frac{\Delta H}{(R+H-\Delta H)(R+H)} \cdot \frac{1}{1-\cos\alpha}. \end{aligned}$$

Then substitute $a\cos\alpha + b$ for $\frac{1}{R+H}$ to get rid of b. Plugging a, b into Equation (7), we get

$$\begin{aligned} \tan(\Delta\theta/2) &= \frac{\Delta H}{(R+H-\Delta H)(R+H)} \cdot \frac{1}{1-\cos\alpha}(R+H)\sin\alpha \\ \tan(\Delta\theta/2) &= \frac{\Delta H}{R+H-\Delta H} \cdot \frac{1+\cos\alpha}{1-\cos^2\alpha} \cdot \sin\alpha \\ \tan(\Delta\theta/2) &= \frac{\Delta H}{R+H-\Delta H} \cdot \frac{1+\cos\alpha}{\sin\alpha}. \end{aligned}$$

Under the assumption that $\Delta\theta$ is small, we expand $\tan\Delta\theta$ with respect to $\Delta\theta$, $\tan(\Delta\theta) = \Delta\theta + 2\Delta\theta^5/15 + ...$ Thus $\tan\Delta\theta \approx \Delta\theta$. From this we have

$$\Delta\theta = \frac{2\Delta H}{R+H-\Delta H} \cdot \frac{1+\cos\alpha}{\sin\alpha}. \tag{8}$$

Assuming α is small, we have $\sin\alpha \approx \alpha$ and $\cos\alpha \approx 1$, so

$$\frac{1+\cos\alpha}{\sin\alpha} \approx \frac{2}{\alpha}.$$

For $R + H \gg \Delta H$, we have

$$\Delta\theta = \frac{\Delta H}{R + H} \cdot \frac{4}{\alpha}. \tag{9}$$

It is necessary to point out, $\Delta\theta$ and α depend on the parameter n, $\alpha = \pi/n$, and $\Delta\theta = 2\pi/n$. The assumption that both angles are small is based on the design principle that n is large. We can compare Figure 2, and Figure 6. In the Figure 2 $n = 4$, whereas in the Figure 6 $n = 2$. We can see the larger the n, the more circle-like the ring will be, and when n goes to infinity, the orbital ring will become a perfect circle. Also, from the comparison, as n increases, ΔH decreases, and we can conclude that ΔH is a function of n. When $n \to \infty$, we have $\Delta H \to 0$, thus $\lim_{n\to\infty} \frac{\Delta H}{R+H} = 0$. We can briefly prove this as follows

Proof:

Rearrange Equation (8), and plug $\alpha = \pi/n$, and $\Delta\theta = 2\pi/n$ to get

$$\frac{(2\pi/n)\sin(\pi/n)}{1 + \cos(\pi/n)} = \frac{\Delta H}{R + H - \Delta H}.$$

Sending $n \to \infty$ on left hand side gives

$$\lim_{n\to\infty} \frac{(2\pi/n)\sin(\pi/n)}{1 + \cos(\pi/n)} = 0.$$

Since $\sin(\pi/n)/[1 + \cos(\pi/n)]$ is bounded, we conclude

$$\lim_{n\to\infty} \frac{\Delta H}{R + H - \Delta H} = 0. \tag{10}$$

Since $R + H$ is constant and ΔH is a function of n, we have the following cases.

Case 1, when $n \to \infty$, $R + H \gg \Delta H$, agrees with Equation (10).

Case 2, when $n \to \infty$, $R + H \ll \Delta H$, $-1 \neq 0$, disagrees with Equation (10).

Case 3, when $n \to \infty$, $\lim_{x\to\infty}(R + H)/\Delta H = (R + H)/\Delta H \neq 0$, disagrees with Equation (10).

All three cases cover the possible relationships between $R + H$ and ΔH. So indeed, we have $\lim_{n\to\infty} \frac{\Delta H}{R+H-\Delta H} = 0 \Rightarrow \lim \frac{\Delta H}{R+H} = 0$. The other direction is obvious, so $\lim_{n\to\infty} \frac{\Delta H}{R+H-\Delta H} = 0 \Leftrightarrow \lim_{n\to\infty} \frac{\Delta H}{R+H} = 0$. We have established our result.

End of proof.

The assumptions we have made are suitable, under the condition that n is large.

Next, we introduce the kinetic force parameter. In Equation (3), set $\phi = \pi/2$, then we have $1/r = b$. When the point moves to the position $\phi = \pi/2$, we call this specific r at the perigee point r_0. If we assume that v_0 is close to the free-running speed at the corresponding orbit, then the ellipse will have a small variation in radius. Based on this assumption, we have $r_0 = R + H$. Then use $b = 1/r_0$ as the connection between the geometric parameters and kinetic parameters. Note that

the centripetal force is provided by gravity, and we get

$$\frac{GMm}{r_0^2} = \frac{v_s^2 m}{r_0},$$

where M is the mass of the earth, m is the mass of the moving point that we are studying here, v_s is the horizontal component of the velocity, and G is the universal gravitational constant. Also note that at the surface of the Earth we have

$$\frac{GM}{R^2} = g.$$

Substituting $GM = R^2 g$ into the previous equation gives

$$\begin{aligned} R^2 g &= v_s^2 r_0 \\ \frac{R^2 g}{v_s^2 r_0^2} &= 1/r_0 \\ &= b \end{aligned}$$

Then substitute a, b back into Equation (4)

$$\begin{aligned} 1/r_0 &= \frac{\Delta H}{r_0(R+H)} \cdot \frac{1}{1-\cos\alpha} + \frac{R^2 g}{v_s^2 r_0^2} \\ \frac{R^2 g}{v_s^2 r_0^2} &= \frac{(R+H)(1-\cos\alpha) - \Delta H}{r_0(R+H)(1-\cos\alpha)} \end{aligned}$$

so that

$$v_s^2 = \frac{R^2 g}{(R+H) - \Delta H/(1-\cos\alpha)}. \tag{11}$$

Since $v_0 \cos\Delta\theta = v_s$, and $\cos\Delta\theta \approx 1$, we have $v_0 = v_s$. Finally, substitute $\Delta\theta$ and v_s^2 into Equation (1), based on Equation (9) and Equation (11) respectively, then we have

$$F_I = \frac{4mgR^2\Delta H}{\alpha(R+H)(R+H-\Delta H/(1-\cos\alpha))}. \tag{12}$$

Noting that $\lim_{\alpha\to 0}(\cos\alpha - 1) = \lim_{\alpha\to 0} -\alpha^2/2$, so $\lim_{\alpha\to 0} 1/(\cos\alpha - 1) = \lim_{\alpha\to 0} 1 - 2/\alpha^2$, we obtain

$$F_I = \frac{4mgR^2\Delta H}{\alpha(R+H)(R+H+\Delta H(1-2/\alpha^2))}.$$

This equation is a bridge between the design parameter, and the lifting capacity. Next, we need to move on to answer the question of stability, safety, etc. We will not address these questions for the regular ORS, but for the PORS in the next chapter. It will lead us to Chapter 3 and the controlling problem.

2.3 The Relationship Between Centrifugal Force & Impulse Supporting Force

The relationship between impulse force and centrifugal force is quite interesting in ORS. When there are just a few Skyhooks in the system, the orbital ring looks like a football with sharp turning angles. However, as the number of the Skyhooks increases in the system, the orbital ring will become more and more circular. Finally, when the number of the Skyhooks goes to infinity, the orbital ring will become a perfect circle, and there will be no impulse at each Skyhook since the turning angle is

0. Thus we can understand the centrifugal force as the extreme case of the impulse supporting force. If we look closely, it is easy to see that the impulse supporting force is actually a way to concentrate the centrifugal force. The summation of magnitude of the impulse supporting force is the integral of the magnitude of centrifugal force. The proof is as follows:

1) First consider an extremely short segment of a rotating ring, shaped as a perfect circle. Let r, A, ρ be the radius of the circular arc, the cross-section area, and the density of the ring. Also let the central angle of this segment be $d\theta$, and the linear speed of the rotating ring be v_0. Then the mass of the segment is

$$m = \rho A r d\theta,$$

and the centrifugal force is

$$dF = \frac{m v_0^2}{r}.$$

Therefore we have

$$dF = \frac{\rho A r d\theta v_0^2}{r}.$$

For the sake of studying the concentration effect, we treat the centrifugal

force as a scalar quantity. Integrating F around the ring gives

$$\begin{aligned} F &= \int_0^{2\pi} \rho A v_0^2 d\theta \\ &= 2\pi\rho A v_0^2. \end{aligned}$$

2) Secondly consider one Skyhook, to which the orbital ring impulses and turns by an angle. Let the turning angle be $\Delta\theta$. Notice that the mass flow of the orbital ring is

$$m = \rho A v_0.$$

It is necessary to point out that the unit for the mass flow is kg/s, The impulse force at each Skyhook F_0, by momentum impulse theorem, is

$$\begin{aligned} F_0 &= m\Delta v \\ &= (\rho A v_0)[2v_0 \sin(\Delta\theta/2)]. \end{aligned}$$

When increasing the number of the Skyhooks to infinity, $\Delta\theta$ will approach 0. In this situation we have $2\sin(\Delta\theta/2) \approx \Delta\theta$, as $\Delta\theta \to 0$, so that

$$F_0 = \Delta\theta\rho A v_0^2.$$

If n represents the number of the Skyhooks in ORS, we have $2\pi = n\Delta\theta$.

The summation of the impulse force as scalar quantity at all Skyhooks is given by

$$\begin{aligned} F &= \sum F_0 \\ &= n\Delta\theta\rho A v_0^2 = 2\pi\rho A v_0^2, \end{aligned}$$

which is the same as the result we obtained from the previous discussion on the centrifugal force from the circular shaped ORS. End of proof.

This proof illustrates that, as a scalar quantity, the total amount of centrifugal force in a circular ring is equivalent to an enclosed piece-wise elliptic ring. Therefore, the enclosed piece-wise elliptic ring is concentrating the evenly distributed centrifugal force along the circle into several symmetrical points, which is beneficial to us, since we want to lift cargo at the Skyhook. A concentrated force would allow a larger lifting capacity for the ORS. This is the very essence of the impulse force supporting technique. In the next chapter, we will discuss the Partial Orbital Ring System, emphasizing more on the evenly distributed centrifugal force than the concentrated force.

3 Partial Orbital Ring System

3.1 Overview of the Partial Orbital Ring System

Although the ORS is a proposed solution to the extremely long lifting cable problem of the Space Elevator, the ORS has several potential disadvantages as well. For example, safety, stability, and the construction problem. After all, a global sized engineering project has

never been seen for human history. [Birch, 1982] proposed a smaller and cheaper ORS that can be built without using rockets. It is named the Partial Orbital Ring System, PORS for short. The shape of a PORS is not a complete circle-liked ring, this is why it is called "partial". Rather, it is an accelerating track, along which the cargoes can be accelerated and sent into the space. The idea of the Lofstrom Loop is based on this concept, and more details concerning the Lofstrom Loop will be discussed in the next chapter. According to [Birch, 1982], the basic structure can be described as follows.

A stream of Particles, or a continuous cable, ejected from one of the ground stations with a sub-orbital velocity, will follow a parabolic trajectory, and can be aimed to come down again at the other ground station. On reaching the ground, the stream can be reversed and sent back to the first ground station alongside its original path. Thus two opposing mass-streams can be formed, and can consist of a single continuous cable. Figures 8 and 9 give images of the PORS and the ground station respectively.

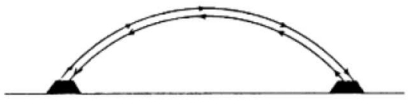

Figure 8: Conceptual PORS [Birch, 1982]

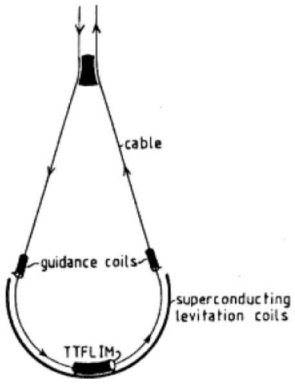

Figure 9: The deflection station [Birch, 1982]

The major difference between a PORS and a standard ORS is that a global rotating Orbital Ring is not necessarily needed in PORS. Rather, PORS uses an arc shaped evacuated tube, inside which a stream of fast moving floating objects can provide centrifugal force for the whole structure and the cargo that moves along it. The basic structure of PORS doesn't necessarily include a Jacob's ladder, or climber. Therefore it is much cheaper to build compared to a full sized ORS. However, just like the standard ORS, PORS must be able to remain stable when a disturbance occurs.

3.2 Stability of a Continuous PORS

In a full sized ORS, the orbital ring works completely outside of the atmosphere, so the friction of air doesn't affect it. However, since most of PORS works inside the atmosphere, where unpredictable disturbances could frequently occur, it is important to study the stability of PORS inside the atmosphere, which is the main topic of this chapter.

The study of the stability problem of a continuous PORS can be summarized as follows: First analyze all the forces in the scenario, introduce a small disturbance as a displacement, build a mathematical model with differential equations, then interpret the solution physically. Figure 10 gives the basic physics scenario for PORS

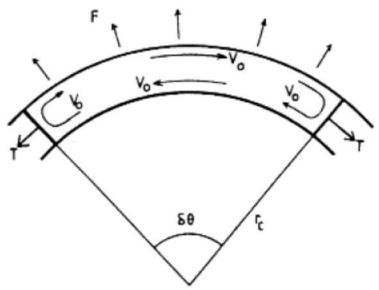

Figure 10: Basic physical scenario of PORS [Birch, 1982]

Here v_0 represent the velocity of the moving stream, T is the tension force at the ends due to rebound, F is the outward centrifugal force per unit length, r_c is the radius of curvature of the arc, and $\Delta\theta$ is the central angle. Then, from the impulse momentum theorem, we obtain

$$T = m_s v_0(2v_0) = 2m_s v_0^2,$$

where $m_s = \rho A$ is the line density of the moving stream inside a vacuum tube, which has the line density m_t. Since, at the end of the arc, the stream flow completely turned around, the changing rate of the

momentum impulse is twice v_0, and F can be represented as follows

$$F = \frac{(2m_s)v_0^2}{r_c}.$$

Therefore we can see $(T/r_c) = F$. This means that if we ignore external force such as gravity, the structure is dynamically neutral. It will not straighten itself or becomes kinked and twisted. However, the gravitational force must be considered, since it has great effect on the structure. We introduce the weight per unit length of the stream and the vacuum tube to be

$$W = (2m_s + m_t)g.$$

We expect the centrifugal force to cancel out the weight of the arc, so $W = F$. Now, introduce a small deviation in radius r, so that $r \to r + dr$. We take a derivative of F with respect to r and get

$$\frac{dF}{dr} = 2m_s[(2v_0/r)\frac{dv_0}{dr} - v_0^2/r^2].$$

Since the moving stream moves in a vertical plane, its angular speed direction is perpendicular to gravity, so that gravity is not able to change the total angular momentum of the system. Based on the

angular momentum conservation law we have

$$dv_0/dr = -v_0/r,$$

which leads to

$$\begin{aligned}\frac{dF}{dr} &= 2m_s[(2v_0/r)(-v_0/r) - v_0^2/r^2] \\ &= 2m_s(-3v_0^2/r^2).\end{aligned}$$

Note $F = 2m_s v_0^2/r_c$ and $W = F$, so

$$dF/dr = -3F/r = -3W/r = -3(2m_s + m_t)g/r.$$

Now, we remove the assumption $W = F$ and introduce a perturbation by setting $P = F - W$, where P is a periodically changing force that makes the ring oscillate once it is disturbed. Also notice that W doesn't vary with respect to r, therefore $dF/dr = dP/dr$. We have

$$dP/dr = -3(2m_s + m_t)g/r. \tag{13}$$

From this formula we see that, as the radius of the arc increases, i.e. the size of the arc increases, the external force P acting on the arc will become less significant, and therefore stable. Solving differential

equation gives

$$P = -3(2m_s + m_t)g \ln r + c. \tag{14}$$

At this point we introduce a finite displacement Z . We change $r = r_0 + dr$ into $r = r_0 + Z$. Then Equation (14) becomes

$$P = -3(2m_s + m_t)g \ln(r_0 + Z) + c. \tag{15}$$

Since P is the restoring force for the oscillation, when the ring is located at its original position, i.e. Z is zero, P should be zero. From this we have $c = 3(2m_s + m_t)g \ln r_0$. We expand P with respect to Z at 0 and get

$$\begin{aligned} P &= -3(2m_s + m_t)g[(\ln r_0 + \frac{1}{r_0 + Z} \cdot Z + ...) - \ln r_0] \\ &= -3(2m_s + m_t)g(\frac{1}{r_0 + Z} \cdot Z + ...). \end{aligned}$$

Take the first approximation to get

$$P = -3(2m_s + m_t)g(\frac{1}{r} \cdot Z). \tag{16}$$

Moreover, by Newton's Second Law

$$P = (2m_s + m_t)\ddot{Z}. \tag{17}$$

Combining Equations (16) and (17) we have

$$\ddot{Z} = -3g(\frac{1}{r} \cdot Z), \tag{18}$$

and solving this differential Equation gives

$$Z = Z_0 e^{i(3g/r)^{1/2}t}. \tag{19}$$

Equation (19) is the relationship between the disturbance and the radius of the arc. Since $e^{i(3g/r)^{1/2}t}$ is bounded, the disturbance will not build up and go out of control as time passes. Also, we have $Z \propto 1/r$, so as the structure and r become larger, the displacement becomes smaller. As a result, the structure can be stabilized based on our model. However, our model can be developed further. More details will be discussed in the next chapter.

In the previous chapter we proved that, to some extent, the impulse supporting force can be treated as a method of concentrating centrifugal force at some points. This is beneficial to us when we want to lift cargo vertically into the space using a Jacob's ladder, since most of the weight will be concentrated at the lifting cable. However, in PORS, we may use the arc shaped ring as a launch track, along which cargo can be accelerated and sent into space. Therefore, there are no special points along the track that require more lifting capacity than other points. As a result, when a PORS structure is used as a launch track, concentrating the centrifugal force will be no longer necessary, hence the emphasis on the centrifugal force in the controlling problem. When it comes to the orbital ring, centrifugal force and impulse supporting force

are actually two aspects of the same kind of force. In Chapter 4 we will explore more details about the control problem using a similar alternative space transportation system, the Lofstrom Loop.

4 The Lofstrom Loop

4.1 Overview of the Lofstrom Loop

From the previous chapters, we know that the fast moving orbital ring can provide a centrifugal force and an impulse supporting force. The centrifugal force supporting effect serves better as an accelerating track, along which cargo can be accelerated and sent into the space. This is where the Lofstrom Loop comes into play. Based on the idea of PORS, Lofstrom developed the accelerating launch track idea with more mathematical and engineering details. Similar to PORS, the partial orbital ring in the Launch Loop is a 2000km wide, 80km high arc. Figures 11 through 13 gives a series of illustrations of the Launch Loop.

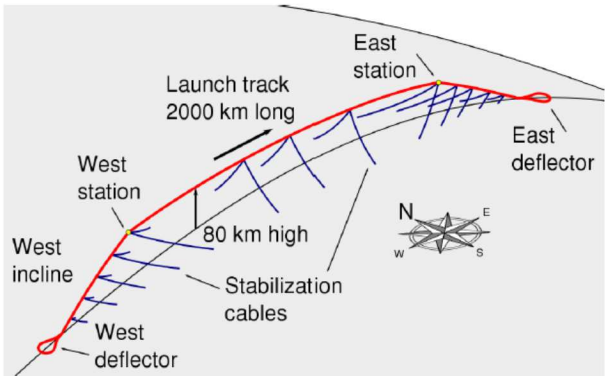

Figure 11: The overview of the Lofstrom's Loop [Lofstrom, 2009]

From the image we can see that the Launch Loop has the following major parts:

1. The Launch track, which is the main part of the Launch Loop, stretches 2000km, and specialized vehicles that carry cargo can be accelerated up to a sufficient speed and be sent into space. The launch path track is suspended on permanent magnets one centimeter below the iron rotor. The launch path track supports sensor and control electronics packages, as well as parachutes to protect sections of track from catastrophic system failure, see Figure 11.

2. The rotor is a fast moving cylinder 5 centimeters in diameter and with walls 2.5 millimeters thick, that floats inside a vacuum sheath. This is the main part of the launch track. The fast moving rotor will provide a centrifugal force, causing tension in the sheath and stabilization cables (see Figure 11), thereby supporting cargo along the track. This rotor circulates around the system once every six minutes, traveling around the ends, up the inclines, down the launch path, then down the incline at the other end. When the rotor reaches the far end of the Launch Loop, it is deflected 180° and returned to complete the cycle, see Figure 11.

3. In front of and behind the launch path are the inclines, which slope down to the surface at angles of 9 to 20 degrees. The forward and reverse rotors of the inclines are surrounded by lightweight vacuum sheaths. Otherwise, friction from the air will cause a loss of energy. The reason for the incline is mainly to control length. If the whole structure kept the same curvature as the launch track, the launch

track would be much longer. The incline is, relatively speaking, a steeper slope that can bring the arc to ground as quickly as possible.

4. Stabilization cables are a set of cables that anchor the launch track to keep it from moving side to side and counter act the weather effect. They require careful control and design, since stabilization failure could result in a catastrophe.

5. Deflector. The upper deflectors are referred to as the "east" and "west" stations. Vehicles are hauled up to the west station and launched . The lower deflector is the place where the rotor gets turned by 180 degrees, and goes back into the launch track again in the reverse direction. The lower deflector is, relatively speaking, easier to design since it is on the surface of some fixed platform, whereas the upper deflector is a challenge, since it is floating halfway in the air.[2]

[2]The above 5 paragraphs are mainly from Lofstrom's paper [Lofstrom, 2009]

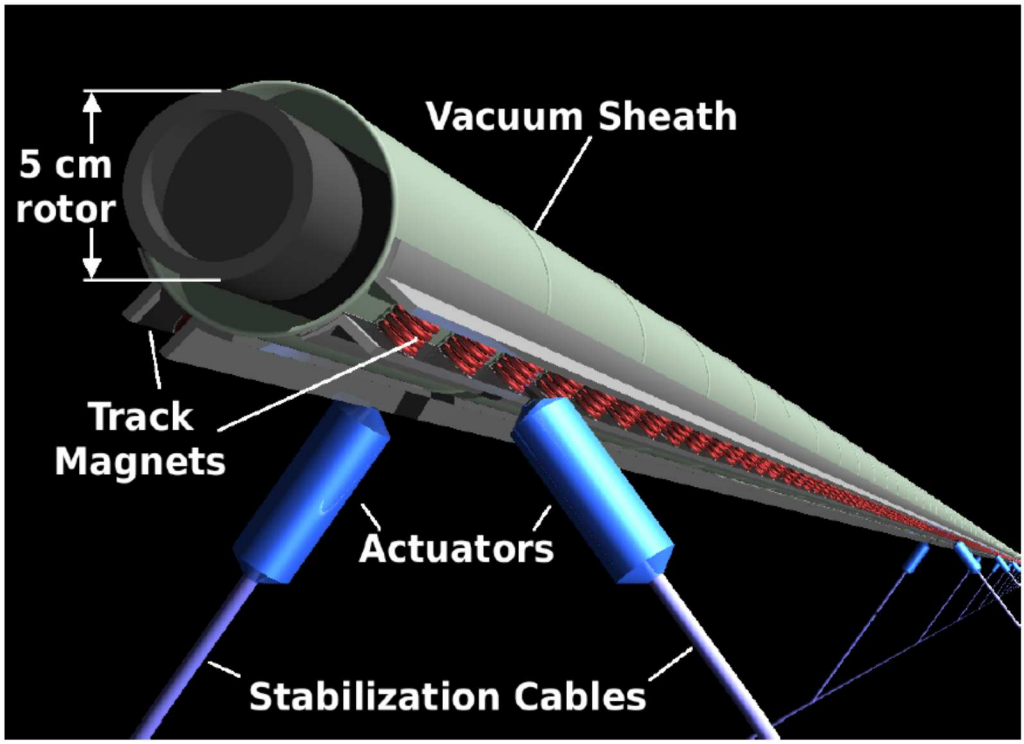

Figure 12: Rotor structure
[Lofstrom, 2009]

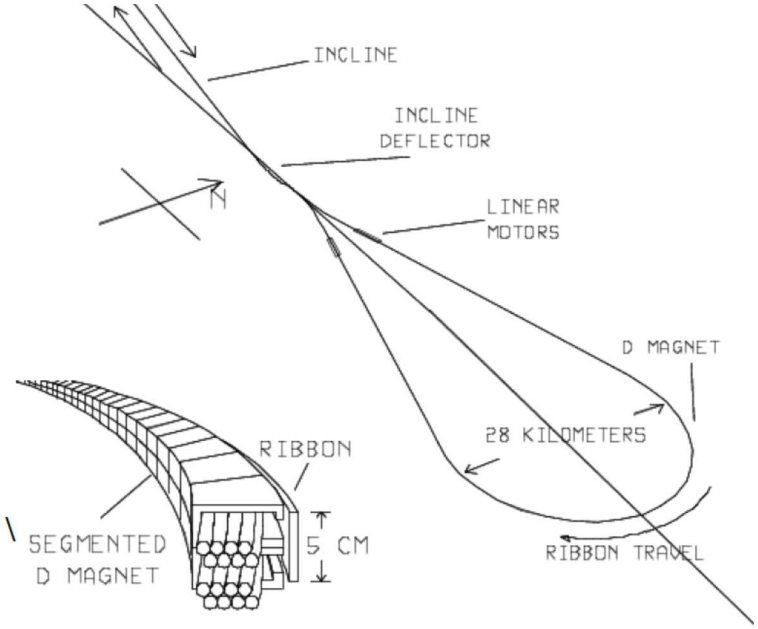

Figure 13: The incline and the deflector
[Lofstrom, 2009]

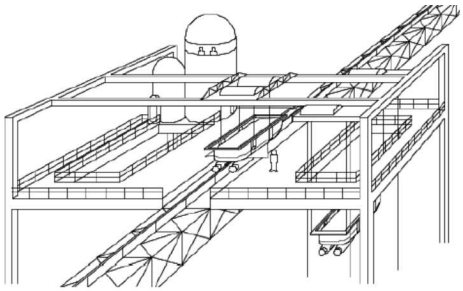

Figure 14: The deflector station
[Lofstrom, 2009]

4.2 Dynamics of Lofstrom's Loop

4.2.1 Rotor & the Impulse Supporting Force

Very similar to the orbital ring in ORS, or the fast moving flow in PORS, the rotor's role in Lofstrom's Loop is to provide a supporting force for the whole structure. Therefore, the model is quite similar to that of ORS and PORS. The formula that relates the lifting force, impact speed and the angle is (the deduction is very similar to Equation (1))

$$F = 2mv^2 \sin(\theta/2), \tag{20}$$

where F is the momentum impulse force, m is the mass of the rotor per length, θ is the deflected angle, and v is the linear speed of the moving rotor. Assume θ is a small angle, we have

$$F = mv^2\theta \tag{21}$$

This is similar to Equation (1). Moreover, other than the concentrated force described by Equation (21), a distributed force can deflect the rotor as well. For example the extra weight of the sheath and magnet that sit on the rotor. When the object is moving at the height r, which is the distance away from the core of the Earth, the relation between

the deflection force, centrifugal force and gravity is

$$f = mv^2/r - mv_0^2/r, \tag{22}$$

where $mv_0^2/r = F_G$, F_G is the gravity at r, and v_0 is the speed of the orbit at r. Since the Lofstrom Loop is very close to the surface of the Earth we have

$$f = [(\frac{v}{v_0})^2 - 1]mv_0^2/r$$
$$f = [(\frac{v}{v_0})^2 - 1]F_G.$$

We approximate $mg = F_G$, and rearrange the formula to obtain

$$f = [(\frac{v}{v_0})^2 - 1]mg. \tag{23}$$

In this form it is easier for us to see the very essence of the distributed deflection force f. Equation (23), is very useful for computing the required speed for a certain load on the launch track. However, Equation (23) is far from enough to describe the physical scenario here. Since there will be a disturbance on the track, we have to discuss the stability of the launch track, which is the real challenge.

4.2.2 The Stability Problem of the Lofstrom Loop & PORS

Before we begin our discussion of the stability of the Lofstrom Loop, a brief review of our discussion on the PORS is beneficial.

In Chapter 2, Section 2, our discussion is based on the question: If we

introduce a disturbance that causes displacement along the radial direction, will the displacement grow as time grows? What is the relationship between the displacement caused by the disturbance acceleration and the radius of the local curvature? The idea is to introduce a correcting current to control the disturbance and prevent failure in the first place. The problem becomes: How can we control this correcting current, so the system will remain stable? What will the function look like? Moreover, Birch's model is built on the assumption that the continuous moving flow has zero stiffness, which is obviously not practical. Lofstrom introduced stiffness to the rotor, and thereby further completed the stability theory of the Lofstrom Loop, and of course, the result could be applied to the PORS.

In order to completely understand the deduction, it is better for us to start from the simpler model in which the rotor is considered to have zero stiffness. Then, based on the simpler model, we introduce the stiffness term to achieve a better model.

4.3 Basic Model for the Controlling Problem

When we talk about the launch track, there are two types, differing by the type magnetic levitation force, attractive or repulsive. To generate a repulsive force between the rotor and the magnets, we have to create eddy currents in the rotor by changing the magnetic flux through the rotor. Obviously, the repulsive force is more stable since the repulsive force would increase when the rotor and magnets come closer together. However, the eddy current would generate tremendous heat due to the limited conductivity of the material of the rotor. Thus, in our model we will consider a launch track using attractive magnetic levitation, where

the rotor floats inside the vacuum sheath surrounded by magnets. We want to discuss whether the rotor could be stabilized or not by some control current.

In our launch track, there is a gap between the rotor and the electromagnets. We don't want the rotor to go beyond this gap and impact the sheath, causing a system failure. If the rotor gets closer to the magnets, the attractive force increases, thereby breaking the balance and causing a failure. Therefore we have to arrange an electronically controlled winding current to counter act this effect.

Assume an electromagnet with magnetic field $B = \mu_0 I/2d$, where I is the original current (compared to the controlling current I_0), μ_0 is the permeability of free space and d is the gap distance between the magnet and the rotor. The magnetic pressure, which is the magnetic attraction per cross-sectional area of the flux, can be described as $B^2/2\mu_0$. Then the attractive force between the two poles of the magnet and the rotor is

$$f = 2W_P \cdot \frac{B^2}{2\mu_0},$$

where W_P is the width of the magnet pole. The width of the pole together with the gap forms the cross-sectional area of the flux $W_P d$, and since the flux passes the gap twice (into and out of the rotor), the

area is $2W_P d$. Substituting $B = \mu_0 I/2d$ into the previous formula gives

$$f = 2W_P \cdot \frac{1}{2\mu_0} \cdot \frac{\mu_0^2 I^2}{4d^2}$$
$$f = W_P \cdot \frac{\mu_0 I^2}{4d^2}.$$

It should be noted that the left hand side of the equation above has the unit N/m instead of N, so f is a linearly distributed force, which makes perfect sense. Our study object is some segment of rotor which has unit length. As the attractive force provides the magnetic centrifugal force (the rotor has a mass per length of m_r), the magnetic centrifugal acceleration a can be computed as follows

$$a = -W_P \cdot \frac{\mu_0 I^2}{4m_r d^2}. \tag{24}$$

We want to use a control current I_0 to counteract the disturbance. When the nominal gap between the rotor and the magnet is d_0, the controlling centrifugal acceleration can be deduced in the same way, and we have

$$a_0 = W_P \cdot \frac{\mu_0 I_0^2}{4m_r d_0^2}. \tag{25}$$

In an ideal situation,$|a_0|$ would equal $|a|$, and since we want to keep a constant gap distance between the rotor and the magnet in the ideal situation, we have $d_0 = d$. As a result, $I_0 = I$. Now we introduce a small nominal perturbation Δd upon d, and we still assume $|a_0| \approx |a|$,

$d_0 \approx d$, hence $I_0 \approx I$. Thus the change in the centrifugal acceleration with gap and current could be given as follows respectively

$$\frac{\partial a}{\partial d} = W_P \cdot \frac{\mu_0 I^2}{2m_r d^3} \approx W_p \cdot \frac{\mu_0 I_0^2}{2m_r d_0^3}$$

$$\frac{\partial a}{\partial I} = W_P \cdot \frac{\mu_0 I}{2m_r d^2} \approx W_P \cdot \frac{\mu_0 I_0}{2m_r d_0^2}.$$

Then, based on Equation (25), substituting in a_0 gives

$$\frac{\partial a}{\partial d} = \frac{2a_0}{d_0}. \tag{26}$$

Note the acceleration a is simply the second derivative of d. For a small perturbation, the local equation of motion can be understood as $\partial a/\partial d = a/d$, so $d \cdot \partial a/\partial d = \ddot{d}$. Based on Equation (26), substitute $\partial a/\partial d$ to obtain

$$\ddot{d} = (2a_0/d_0)d. \tag{27}$$

Let $A = 2a_0/d_0$, then Equation (27) becomes $\ddot{d} = Ad$, so the characteristic function is $r^2 = A$. The roots for the characteristic function are $r_{1,2} = \pm\sqrt{A}$. Therefore the solution to Equation (27) is given by $d = c_1 e^{\sqrt{A}t} + c_2 e^{-\sqrt{A}t}$. Since we assume the gap d shouldn't deviate too much from d_0, d is bounded as $t \to \infty$, so $c_1 = 0$. When $t = 0$, we should have $d = d_0$. So that, from the initial condition,

$d_0 = c_2$. Thus $A = 2a_0/d_0$ and the solution to Equation (27) becomes

$$d = d_0 e^{-\sqrt{2a_0/d_0}t}. \tag{28}$$

This solution doesn't take the stiffness of the rotor into consideration. The stiffness of the rotor shouldn't be ignored, since the rotor is made up of many long segments of iron cylinders. Thus we introduce a stiffness term into our model. We will obtain a more complicated equation, which we will explore in the next section.

4.4 A More Advanced Model for the Controlling Problem

In the previous section, we built a basic mathematical model in which the rotor is considered as some soft stiffless material, but this is far from the truth, since the rotor is actually made of iron. So it is necessary to introduce an additional bending force term into our model, to make it accurate.

We perform the calculation in a moving frame of reference $x - x_0 = vt$. Let E be the Young's modulus, and I_b be the bending moment. According to the beam equation, the bending force can be expressed as

$$f_b = -E \cdot I_b \frac{\partial^4 d}{\partial x^4}. \tag{29}$$

Let R_o be the outer radius, R_i be the inner radius, h be the thickness of the cylindrical shell, and R_a be the average radius of R_o and R_i, then

the bending moment for a cylindrical shell is given by

$$I_b = \frac{\pi}{4}(R_o^4 - R_i^4). \tag{30}$$

Expanding we obtain

$$\begin{aligned} I_b &= \frac{\pi}{4}(R_o^4 - R_i^4) \\ &= \frac{\pi}{4}(R_o^2 + R_i^2)(R_o + R_i)(R_o - R_i) \\ &= \frac{\pi}{4}(R_o^2 + R_i^2)(2R_a)h \\ &\approx \frac{\pi}{4}(2R_a^2)(2R_a)h. \end{aligned}$$

As a result

$$I_b = \pi R_a^3 h. \tag{31}$$

The reason we can approximate $R_o^2 + R_i^2$ with $2R_a^2$ is because the thickness is small compared to the radius of the cylinder, but we will compute the error in order to get a better understanding of how good this approximation is. According to Lofstrom, the thickness of the cylindrical shell is only 2.5 mm, and the outer radius is 25 mm. Computing the difference between $R_o^2 + R_i^2$ and $2R_a^2$ we have

$$\begin{aligned} R_o^2 + R_i^2 - 2R_a^2 &= (R_a + h/2)^2 + (R_a - h/2)^2 - 2R_a^2 \\ &= h^2/2, \end{aligned}$$

so, as a percentage error, we have $(h^2/2)/(R_o^2 + R_i^2)$. According to the data provided by Lofstrom in his design, $h^2/2 = 3.125$ and $R_o^2 + R_i^2 = 1131.25$, so the percentage error is 0.276% which is an acceptable system error. Substitute Equation (31) into (29) to get

$$f_b = -E \cdot \pi R_a^3 h \cdot \frac{\partial^4 d}{\partial x^4}. \tag{32}$$

Also note that, under the assumption that the thickness is relatively small compared to the radius, the unit length mass of the rotor can be expressed as

$$m_r \approx 2\pi\rho h \cdot R_a. \tag{33}$$

By Newton's Second Law (take f_b divided by m_r), the corresponding acceleration is given by

$$a_b = \left(\frac{ER_a^2}{2\rho}\right)\frac{\partial^4 d}{\partial x^4}. \tag{34}$$

Combining Equation (27) with the stiffness term described by Equation (34), the differential equation describing the rotor becomes

$$\frac{\partial^2 d}{\partial t^2} = \left(\frac{2a_0}{d_0}\right)d - \left(\frac{ER_a^2}{2\rho}\right)\frac{\partial^4 d}{\partial x^4}. \tag{35}$$

First let $A = 2a_0/d_0$, and $B = ER_a^2/2\rho$, then Equation (35) can be transformed into

$$\frac{\partial^2 d}{\partial t^2} = Ad - B\frac{\partial^4 d}{\partial x^4}. \tag{36}$$

Using the variable separation method, assume $d(x,t) = T(t)X(x)$, then Equation (36) becomes

$$\ddot{T}X = A \cdot TX - B \cdot TX^{(4)}. \tag{37}$$

Dividing both sides of the equation by $T(t)X(x)$ we have

$$\ddot{T}/T = A - B \cdot X^{(4)}/X. \tag{38}$$

Note A and B are constants, i.e. they are not functions of t or x. Thus we should have $\ddot{T}/T = -\mu$, where μ is a constant. Therefore $-\mu = A - B \cdot X^{(4)}/X$. Rearranging these two equations we get

$$\ddot{T} + \mu T = 0 \tag{39}$$

$$X^{(4)} + \frac{A-\mu}{B}X = 0. \tag{40}$$

Solve Equation (39) by the characteristic method, i.e. we assume the solution is proportional to e^{rt} where r is the root to the characteristic equation

$$r^2 + \mu = 0. \tag{41}$$

If we assume μ>0, then the roots of Equation (41) are given by $r_{1,2} = \pm\sqrt{\mu}$, so the solution to Equation (39) can be expressed as

$$T(t) = c_1 e^{\sqrt{\mu}t} + c_2 e^{-\sqrt{\mu}t}.$$

Solving Equation (40) using a similar method gives

$$r^4 + \frac{\mu - A}{B} = 0. \tag{42}$$

Let $\lambda = (A - \mu)/B = r^4$, which is always positive, then the roots for Equation (42) are $r_1 = \lambda^{1/4}$, $r_2 = -\lambda^{1/4}$, $r_3 = i\lambda^{1/4}$, $r_4 = -i\lambda^{1/4}$. Thus the solution to Equation (42) can be expressed as

$$X(x) = c_3 e^{x\lambda^{1/4}} + c_4 e^{-x\lambda^{1/4}} + c_5 e^{ix\lambda^{1/4}} + c_6 e^{-ix\lambda^{1/4}}.$$

Combine $X(x)$ with $T(t)$ to get the solution for $d(x,t)$

$$\begin{aligned} d(x,t) &= X(x)T(t) \\ &= [c_3 e^{x\lambda^{1/4}} + c_4 e^{-x\lambda^{1/4}} + c_5 e^{ix\lambda^{1/4}} + c_6 e^{-ix\lambda^{1/4}}][c_1 e^{\sqrt{\mu}t} + c_2 e^{-\sqrt{\mu}t}] \\ &= c_1 c_3 e^{x\lambda^{1/4}+\sqrt{\mu}t} + c_1 c_4 e^{-x\lambda^{1/4}+\sqrt{\mu}t} + c_1 c_5 e^{ix\lambda^{1/4}+\sqrt{\mu}t} + c_1 c_6 e^{-ix\lambda^{1/4}+\sqrt{\mu}t} \\ &+ c_2 c_3 e^{x\lambda^{1/4}-\sqrt{\mu}t} + c_2 c_4 e^{-x\lambda^{1/4}-\sqrt{\mu}t} + c_2 c_5 e^{ix\lambda^{1/4}-\sqrt{\mu}t} + c_2 c_6 e^{-ix\lambda^{1/4}-\sqrt{\mu}t}. \end{aligned}$$

But this solution is based on the assumption that $\mu > 0$, or $\mu = 0$ there is also a possibility that $\mu < 0$. Thus when $\mu < 0$, solve Equation (41)

to get $r_{1,2} = \pm i\sqrt{-\mu}$. The solution to the Equation (37) becomes

$$d(x,t) = c_1c_3e^{x\lambda^{1/4}+i\sqrt{-\mu}t} + c_1c_4e^{-x\lambda^{1/4}+i\sqrt{-\mu}t} + c_1c_5e^{ix\lambda^{1/4}+i\sqrt{-\mu}t} + c_1c_6e^{-ix\lambda^{1/4}+i\sqrt{-\mu}t}$$
$$+ c_2c_3e^{x\lambda^{1/4}-i\sqrt{-\mu}t} + c_2c_4e^{-x\lambda^{1/4}-i\sqrt{-\mu}t} + c_2c_5e^{ix\lambda^{1/4}-i\sqrt{-\mu}t} + c_2c_6e^{-ix\lambda^{1/4}-i\sqrt{-\mu}t}.$$

Now, based on the physical scenario, we study the options for our control parameters μ and λ.

First study μ. If $\mu > 0$, then $T(t) = c_1e^{\sqrt{\mu}t} + c_2e^{-\sqrt{\mu}t}$, so $T(t)$ has the potential to grow unbounded as time goes to infinity. Therefore choose $\mu < 0$, i.e. $T(t) = c_1e^{i\sqrt{-\mu}t} + c_2e^{-i\sqrt{-\mu}t}$, where $T(t)$ will be bounded.

Then study the four roots for $\lambda = r^4$. For root $\lambda^{1/4}$, terms $c_1c_3e^{x\lambda^{1/4}+i\sqrt{-\mu}t}$ and $c_2c_3e^{x\lambda^{1/4}-i\sqrt{-\mu}t}$ will be unbounded as $x \to \infty$, so consider root $-\lambda^{1/4}$. It seems the corresponding term $c_1c_4e^{-x\lambda^{1/4}+i\sqrt{-\mu}t}$ and $c_2c_4e^{-x\lambda^{1/4}-i\sqrt{-\mu}t}$ would be bounded as $x \to \infty$ and $t \to \infty$. This can be understood as the disturbance spreading out as a wave going infinitely far from the disturbance source. However, since the rotor is actually going in a loop inside the launch track tube, the rotor will be turned around at the east or west deflector, see Figure 13, i.e. the infinitely far assumption doesn't hold. The only options left are $\pm i\lambda^{1/4}$ and obviously in terms $c_1c_5e^{ix\lambda^{1/4}+i\sqrt{-\mu}t}$, $c_1c_6e^{-ix\lambda^{1/4}+i\sqrt{-\mu}t}$, $c_2c_5e^{ix\lambda^{1/4}-i\sqrt{-\mu}t}$ and $c_2c_6e^{-ix\lambda^{1/4}-i\sqrt{-\mu}t}$ the exponents are imaginary, therefore all of them are bounded. As a result, we choose $\pm i\lambda^{1/4}$. Our solution becomes $d(x,t) =$
$c_1c_5e^{ix\lambda^{1/4}+i\sqrt{-\mu}t} + c_1c_6e^{-ix\lambda^{1/4}+i\sqrt{-\mu}t} + c_2c_5e^{ix\lambda^{1/4}-i\sqrt{-\mu}t} + c_2c_6e^{-ix\lambda^{1/4}-i\sqrt{-\mu}t}$.

Next, in order to find the relationship between μ and λ, plug our solution into the differential equation. Letting $\sqrt{-\mu} = \omega$, and $k = \lambda^{1/4}$,

we write our solution as $d(x,t) = d_0 e^{i(\omega t - kx)}$. Here ω can be explained as the angular frequency, and k is the wave-number, related to the wavelength. We can see, if $k = 0$, the stiffness term vanishes, i.e. the rotor is made of extremely soft material, and the solution becomes $d(x,t) = d_0 e^{i\omega t}$. This is consistent with the solution for the basic model from last section. As k increases from zero, the stiffness of the rotor increases. In order to see this effect in detail, we plug $d(x,t) = d_0 e^{i(\omega t - kx)}$ into Equation (35) which gives

$$-\omega^2 = \left(\frac{2a_0}{d_0}\right) - \left(\frac{ER_a^2}{2\rho}\right) k^4. \tag{43}$$

With $k = 2\pi/l$, we have $-\omega^2 = (2a_0/d_0) - \left(ER_a^2/2\rho\right)(2\pi)^4/l^4$. Note that $\mu = -\omega^2$, and we know $\mu < 0$, therefore we obtain the following inequality

$$\left(\frac{2a_0}{d_0}\right) - \left(\frac{ER_a^2}{2\rho}\right)\left(\frac{2\pi}{l}\right)^4 < 0.$$

Thus the restriction for l is given by

$$l < 2\pi \left(\frac{d_0 E R_a^2}{4a_0\rho}\right)^{1/4}. \tag{44}$$

With initial data $E/\rho = 5177\text{m/s}$, $d_0 = 0.01\text{m}$, $R_a = 0.25\text{m}$, $a_0 = 9.81 m/s^2$, the maximum wave-length allowed is 144 cm, which is not impossible to control.

In our model, we are merely stating that for a one time displacement, the oscillation of the system will not grow without bound over time. But

by looking at the solution, the imaginary exponential structure suggests that the disturbance doesn't vanish. The oscillation of the rotor will not be damped out for external reasons because the rotor moves inside the vacuum tube. Therefore, the energy of the oscillation will build up, and cause a failure of the system. A damping system is required here, which might be a good potential research topic for the future.

5 Summary and Future Work

5.1 The Two aspects

In the previous four chapters, we have introduced a series of alternate space transportation systems. From the Space Elevator to the Launch Loop. They are all different types of large scale space transportation system. The Space Elevator and the ORS fall into the category of lifting-cable-based systems, whereas the Lofstrom Launch Loop and the PORS fall into the category of launch-track-based systems. In Chapter 2 Section 3 we concluded that the impulse supporting force and the centrifugal force are two different aspects of the same kind of force. The connection here is that the impulse supporting can "concentrate" the evenly distributed centrifugal force onto several points. Thus at those specific points, the centrifugal force is extremely large and can be used to support the lifting cable and the cargo on it.

But why are we interested in both kinds of applications? The lifting-cable-based system specializes in lifting. It can be used to lift the cargo vertically into space in a low-speed and low-cost manner, but it cannot accelerate the cargo to a high linear speed. Whereas the launch-track-based system can be used to accelerate the cargo to a high

linear speed along the launch track. But according to [Lofstrom, 2009], the launch track is 80 km, and 2000 km wide, which is very inefficient in terms of lifting altitude. Therefore, to optimize these two effects would be a good direction for future work.

5.2 The Controlling Problem

Our discussion on the controlling problem in Chapters 3 and 4 shows that, for one time disturbances, the system can be controlled but the disturbing wave won't damp out. However, for multiple strikes, the energy will build up. Further design of a damping system is required. Additionally, we can see the control system requires a whole set of controlling electromagnets along the 2000 km launch track. This is of great cost, since other than a huge investment of building such a controlling system, the controlling current will consume lots of energy. Therefore, future work on the controlling problem should focus on how to build a launch track that does not require an along-track controlling system. There are also many other systems to be explored. Hopefully this breathtaking engineering project will draw more attention, and one day become a reality, starting a new era of human history in the near future.

References

Paul Birch. Orbital ring systems and jacob's ladders i. *Journal of the British Interplanetary Society*, 35(475-497), 1982.

Paul Birch. Orbital ring systems and jacob's ladders ii. *Journal of the British Interplanetary Society*, 36(115-128), 1983a.

Paul Birch. Orbital ring systems and jacob's ladders iii. *Journal of the British Interplanetary Society*, 36(231-238), 1983b.

Randall D. Knight. *Physics for Scientists and Engineers: A Strategic Approach with Modern Physics and Mastering Physics*. Addison Wesley, 2007.

Keith Lofstrom. The launch loop. 2009.